Article

Cross-sectional Analysis of Beams Subjected to Saint-Venant Torsion Using the Green's Theorem and the Finite Difference Method

Valentin Fogang

Civil Engineer, C/o BUNS Sarl, P.O Box 1130, Yaounde, Cameroon; valentin.fogang@bunscameroun.com

valentinfogang@yahoo.de   ORCID iD   https://orcid.org/0000-0003-1256-9862

Abstract: This paper presents an approach to the elastic analysis of beams subjected to Saint-Venant torsion using Green's theorem and the finite difference method (FDM). The Saint-Venant torsion of beams, also called free torsion or unrestrained torsion, is characterized by the absence of axial stresses due to torsion; only shear stresses are developed. The solution to this torsion problem consists of finding a stress function that satisfies the governing equation and the boundary conditions. The FDM is an approximate method for solving problems described with differential or partial differential equations; it does not involve solving differential equations, equations are formulated with values at selected nodes of the structure. In this paper, the beam's cross-section was discretized using a two-dimensional grid and additional nodes were introduced at the boundaries. The introduction of additional nodes allowed us to apply the governing equations at boundary nodes and satisfy the boundary conditions. Beam's cross-sections of various shapes and openings were analyzed using this model; shear stresses, torsion constant, and warping were determined. Furthermore, beams with thin-walled closed sections, single-cell or multiple-cell, were analyzed using the stress function whereby the linear distribution of the shear stresses over the thickness was considered; closed-form solutions for shear stresses and torsion constant were presented. For rectangular cross-sections, the results obtained in this study showed good agreement with the exact results, and the accuracy was increased through a grid refinement. For thin-walled closed sections it was noted that the maximal shear stress in the midline occurs at the position with the smallest thickness, which is in agreement with Bredt's analysis, but the maximal shear stress in the cross-section did not necessarily occur at that position; moreover, the values of torsion constant were higher than those calculated using Bredt's analysis

Keywords: Theory of elasticity; Saint-Venant torsion; Green's theorem; finite difference method; additional nodes; thin-walled sections; cross-section with openings; warping

1.   Introduction

This paper describes the application of Fogang's model [1] based on the finite difference method (FDM), used for the homogeneous Euler−Bernoulli beam, to the elastic analysis of beams subjected to Saint-Venant torsion. The Saint-Venant torsion is characterized by the absence of axial stresses due to torsion; only shear stresses are developed. The correct solution of the problem of torsion of prismatical beams was given by Saint-Venant [2]; he made assumptions on

Cross-sectional Analysis of Beams Subjected to Saint-Venant Torsion

the deformation of the twisted bar that could satisfy the equations of equilibrium and the boundary conditions. Bredt [3] derived formulas for the torsional analysis of thin-walled bars; these formulas form a basis for the calculation of shear stresses and deformations in components with closed, thin-walled hollow cross-sections under pure torsional loading. Prandtl [4] introduced a stress function in terms of which the shear stresses were defined. Therefore, the solution of the torsion problem consists of finding a stress function which satisfies the governing equation and the boundary conditions. Analytical solutions of the stress function are available for beams with elliptical cross-sections, equilateral triangle and several other shapes; furthermore, the torsional problem was solved for rectangular cross-section using infinite trigonometric series. However, analytical solutions of the Saint-Venant torsion are only suitable for simple cross-sections; therefore, numerical methods to evaluate the torsional behavior of complicated cross-sections are indispensable. Numerical methods such as energy methods were considered by numerous authors i.e. Ritz [5] and Trefftz [6]; the stress function was approximately determined from the minimum condition of the strain energy of the twisted beam. Various studies have focused on the analysis of beams under unrestrained torsion. Pluzsik et al. [7] presented a theory for thin-walled, closed section, orthotropic beams which takes into account the shear deformation in restrained warping induced torque; the analytical ("exact") solution of simply supported beams subjected to a sinusoidal load was developed for this purpose. Pan et al. [8] presented a matrix stiffness method for the torsion and warping analysis of beam-columns in order to investigate the exact element torsional stiffness considering warping deformations; the equilibrium analysis of an axial-loaded torsion member was conducted, and the torsion-warping problem was solved based on a general solution of the established governing differential equation for the angle of twist. Pavazza et al. [9] presented a novel theory of torsion of thin walled beams ("shear deformable beams") of arbitrary open cross-sections with influence of shear; the theory is based on the classical Vlasov's theory of thin-walled beams of open cross-section, as well on the Timoshenko's beam bending theory. Choi & Kim [10] proposed a higher-order Vlasov torsion theory that not only includes as many torsion-related modes as desired but also provides the explicit forces–kinematic variables–stresses relationships that are fully consistent with those by the Vlasov theory. Amulu & Ezeagu [11] investigated the effect of combined actions of torsion moments, bending moments and shear forces in reinforced concrete beams with concrete compressive strength of $30N/mm^2$; the ultimate torsion moments, bending moments, and shear forces of the beams were determined experimentally. Tran [12] used isoparametric eight-noded quadrilateral elements in order to improve Gruttmann's isoparametric four-noded quadrilateral elements; MATLAB was the language for programming the numerical method.

In this paper the torsion problem of beams with solid cross-sections was solved using FDM. The cross-sections were discretized with a two-dimensional grid and additional nodes were introduced at the boundaries. The introduction of additional nodes allowed us to apply the governing equations at boundary nodes and to satisfy the boundary conditions. Sections with openings were also analyzed. So, the values of the stress function at nodes were determined and thereafter the shear stresses, torsion constant, and warping. Beams with thin-walled closed sections were analyzed using the stress function whereby the linear distribution of the shear stresses over the thickness was considered; closed form solutions for shear stresses and torsion constant were presented and compared to those of Bredt [3].

Cross-sectional Analysis of Beams Subjected to Saint-Venant Torsion

2. Materials and methods

2.1 Linear elasticity of unrestrained torsion of beams

The axis convention in the cross-section is represented in Figure 1, whereas the x-axis is the longitudinal beam's axis.
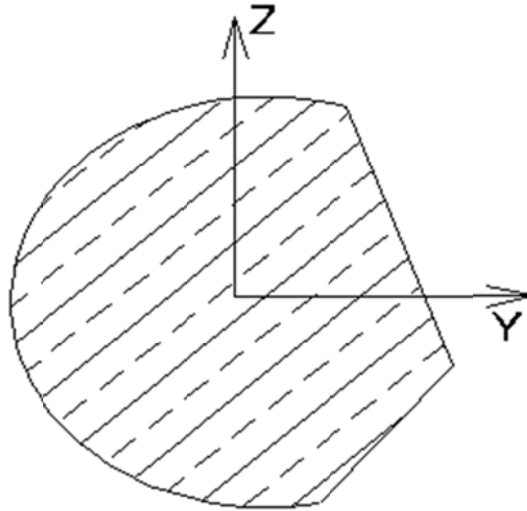

Figure 1.   Axis convention within the beam's cross-section

The equations in this section are related to the theory of linear elasticity of beams. The displacements in x-, y-, and z-direction are denoted by u(x,y,z), v(x,y,z), and w(x,y,z), respectively, and the rotation of cross-section or angle of twist (positive anticlockwise) is denoted by θ(x). The shearing strains γ_{xy} and γ_{xz} are related to the displacements as follows:

$$\gamma_{xy} = \frac{\partial u}{\partial y} + \frac{\partial v}{\partial x}, \qquad \gamma_{xz} = \frac{\partial u}{\partial z} + \frac{\partial w}{\partial x} \tag{1a, b}$$

The cross-sections are assumed to rotate about an axis through the center of torsion $T\,(y_T, z_T)$ (which is equivalent to the shear center). Therefore, the displacements v(x,y,z) and w(x,y,z) are related to the angle of twist θ(x) as follows

$$v = -(z - z_T)\theta, \qquad w = (y - y_T)\theta \tag{2a, b}$$

Combining Equations (1a-b) and (2a-b) yields the stress strains relationships

$$\tau_{xy} = G\left(\frac{\partial u}{\partial y} - (z - z_T)\frac{d\theta}{dx}\right), \qquad \tau_{xz} = G\left(\frac{\partial u}{\partial z} + (y - y_T)\frac{d\theta}{dx}\right) \tag{3a, b}$$

where G is the shear modulus. Combining Equations (3a) and (3b) yields following relationship between the shear stresses and the rotation θ(x)

$$\frac{\partial \tau_{xy}}{\partial z} - \frac{\partial \tau_{xz}}{\partial y} = -2G\frac{d\theta}{dx} \tag{4}$$

Cross-sectional Analysis of Beams Subjected to Saint-Venant Torsion

Recalling that axial stresses do not occur in the beam subjected to unrestrained torsion, the equilibrium equation in x-direction applied to an infinitesimal beam element with dimensions dx, dy, and dz yields

$$\frac{\partial \tau_{xy}}{\partial y} + \frac{\partial \tau_{xz}}{\partial z} = 0 \tag{5}$$

Prandtl [4] introduced a stress function $\phi(x,y,z)$, defined in terms of stress components as follows

$$\tau_{xy} = \frac{\partial \phi}{\partial z}, \qquad \tau_{xz} = -\frac{\partial \phi}{\partial y} \tag{6}$$

It is noted that Equations (6) satisfy the equilibrium equation (5). Substituting Equations (6) into (4) yields the following condition to be satisfied by the stress function $\phi(x,y,z)$

$$\frac{\partial^2 \phi}{\partial y^2} + \frac{\partial^2 \phi}{\partial z^2} = -2G\frac{d\theta}{dx} \tag{7}$$

The analysis is then reduced of determining the stress function.

Let us consider an infinitesimal beam element at the boundary with dimensions dx, -dy, and dz. The outer normal **n** to the boundary makes an angle α with the +y-axis, as represented in Figure 2.
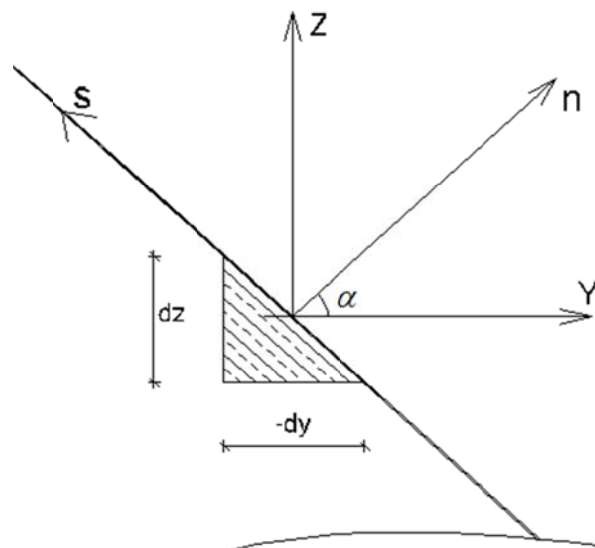

Figure 2 Infinitesimal beam element at boundary

Considering that axial stresses do not occur, the equilibrium equation applied to the beam element along the x-axis combined with Equation (6) yields

$$-\tau_{xz}\left(-dy\right)\times dx - \tau_{xy}dz\times dx = 0$$

$$\rightarrow \frac{\partial \phi}{\partial y}dy + \frac{\partial \phi}{\partial z}dz = 0 \rightarrow d\phi = 0 \tag{8}$$

Cross-sectional Analysis of Beams Subjected to Saint-Venant Torsion

This means that the stress function $\phi(x,y,z)$ is constant along the boundary of the cross-section. Observing that $\sin\alpha = -dy/ds$ and $\cos\alpha = dz/ds$, the shearing stress component τ_t at the boundary directed along the tangent is

$$\tau_t = -\tau_{xy}\sin\alpha + \tau_{xz}\cos\alpha = -\frac{\partial\phi}{\partial z}\sin\alpha - \frac{\partial\phi}{\partial y}\cos\alpha = \frac{\partial\phi}{\partial z}\frac{dy}{ds} - \frac{\partial\phi}{\partial y}\frac{dz}{ds} \tag{9a}$$

Likewise, the shearing stress component τ_n at the boundary directed along the outer normal to the boundary is

$$\tau_n = \tau_{xy}\cos\alpha + \tau_{xz}\sin\alpha = \frac{\partial\phi}{\partial z}\cos\alpha - \frac{\partial\phi}{\partial y}\sin\alpha = \frac{\partial\phi}{\partial z}\frac{dz}{ds} + \frac{\partial\phi}{\partial y}\frac{dy}{ds} \tag{9b}$$

Observing Equation (8), the shearing stress component τ_n is zero; this is in agreement with the condition of stress free outer surfaces. Therefore, the resultant shearing stress at the boundary is τ_t. Let us recall the Green's theorem which relates a line integral around a closed curve B to a double integral over the plane region A bounded by B

$$\oint_B \left[Ldy + Mdz \right] = \iint_A \left[\frac{\partial M}{\partial y} - \frac{\partial L}{\partial z} \right] dydz \tag{10}$$

whereby L and M are functions defined on the region A and the path of integration along B is anticlockwise.

Recalling that the stress function has a constant value ϕ_B at the boundary, the Green's theorem shows as follows that the resultant shear forces are zero

$$\iint \tau_{xz}dydz = \iint -\frac{\partial\phi}{\partial y}dydz = -\oint_B \phi dz = -\phi_B \oint_B dz = 0$$

$$\iint \tau_{xy}dydz = \iint \frac{\partial\phi}{\partial z}dydz = -\oint_B \phi dy = -\phi_B \oint_B dz = 0 \tag{11}$$

where the line integrals are taken around the closed boundary B of the cross-section. Using Equations (6) and (11), the torque is then given by

$$M_t = \iint \left[\tau_{xz}(y - y_T) - \tau_{xy}(z - z_T) \right]dydz = \iint \left[-\frac{\partial\phi}{\partial y}y - \frac{\partial\phi}{\partial z}z \right]dydz \tag{12a}$$

The derivatives of ϕy with respect to y and ϕz with respect to z, respectively, are given by

$$\frac{\partial[\phi y]}{\partial y} = \frac{\partial\phi}{\partial y}y + \phi, \qquad \frac{\partial[\phi z]}{\partial z} = \frac{\partial\phi}{\partial z}z + \phi \tag{12b}$$

Cross-sectional Analysis of Beams Subjected to Saint-Venant Torsion

Substituting Equations (12b) into (12a) yields

$$M_t = 2\iint \phi \, dydz - \iint \left[\frac{\partial[\phi y]}{\partial y} + \frac{\partial[\phi z]}{\partial z} \right] dydz \tag{12c}$$

In the case of cross-sections without openings and recalling that the stress function has a constant value ϕ_B at the boundary, the Green's theorem applied to the second term at the right-hand side of Equation (12c) is given by

$$\iint \left[\frac{\partial[\phi y]}{\partial y} + \frac{\partial[\phi z]}{\partial z} \right] dydz = \oint_B \left[\phi y \, dz - \phi z \, dy \right] = \phi_B \oint_B \left[y \, dz - z \, dy \right] = 2\phi_B A_B \tag{12d}$$

where A_B is the area enclosed by the outer boundary of the cross-section. Let us express the stress function as follows

$$\phi(x, y, z) = \phi_B + \phi^*(x, y, z) \tag{12e}$$

with the function ϕ^* being zero along the boundary and satisfying Equation (7). Substituting Equations (12d) and (12e) into (12c) yields

$$M_t = 2\iint \phi^* \, dydz \tag{12f}$$

Therefore, for a beam's cross-section without openings the expression of the torque is independent of the value ϕ_B of the stress function at the boundary. Furthermore, Equations (12a-f) show that half the torque is due to the stress component τ_{xy} and the other half to τ_{xz}. For simplification purpose, a modified stress function $\psi(y,z)$ is defined

$$\phi^*(x, y, z) = G \frac{d\theta}{dx} \times \psi(y, z) \tag{13a}$$

Thus, the function $\psi(y,z)$ is zero along the boundary. Substituting Equations (13a) and (12e) into (7) and (6) yields

$$\frac{\partial^2 \psi}{\partial y^2} + \frac{\partial^2 \psi}{\partial z^2} = -2 \tag{13b}$$

$$\tau_{xy} = G \frac{d\theta}{dx} \times \frac{\partial \psi}{\partial z}, \qquad \tau_{xz} = -G \frac{d\theta}{dx} \times \frac{\partial \psi}{\partial y}$$

The torsional stiffness GI_t is related to the torque M_t and the angle of twist $\theta(x)$ as follows

$$M_t = GI_t \frac{d\theta}{dx} \tag{13c}$$

Combining Equations (12f), (13a), and (13c) yields the torsion constant I_t

Cross-sectional Analysis of Beams Subjected to Saint-Venant Torsion

$$I_t = 2\iint \psi \, dy \, dz \tag{13d}$$

In the case of cross-sections having openings Equation (12d) becomes

$$\iint \left[\frac{\partial[\phi y]}{\partial y} + \frac{\partial[\phi z]}{\partial z} \right] dy\,dz = 2\phi_B A_B - \sum_i 2\phi_i A_i \tag{14a}$$

where A_i are the areas enclosed by the openings i and ϕ_i the constant values of the stress function along the boundary of the opening i. Combining Equations (12c, e) and (14a) yields

$$M_t = 2\iint \phi^* dy\,dz + \sum_i 2\phi_i A_i \tag{14b}$$

Observing that $\phi_i = \phi_B + \phi^*_i$, we set ϕ_B to zero and combine Equations (13a, c) and (14b) to obtain the torsion constant

$$I_t = 2\iint_A \psi \, dy\,dz + 2\sum_i \psi_i A_i \tag{14c}$$

Equation (14c) can be found in Dieker [13].

2.2 Finite difference approximations

For simplification purpose, the analysis will be conducted in the following with the modified stress function $\psi(y,z)$. The analysis is then governed by Equation (13b-1). This equation has second order derivatives; consequently, the function $\psi(y,z)$ is approximated around the node of interest $\dot{\text{i}}$ as a second degree polynomial in each direction. The unknown at any node is the value ψ_i of the modified stress function.

Given the grid spacings $\Delta y = h$ and $\Delta z = \lambda h$ in y- and z-direction, respectively. The finite difference approximations (FDAs) for the first and second derivatives are then given by

$$\left.\frac{\partial^2 \psi}{\partial y^2}\right|_{i-1} = \left.\frac{\partial^2 \psi}{\partial y^2}\right|_i = \left.\frac{\partial^2 \psi}{\partial y^2}\right|_{i+1} = \frac{\psi_{i-1} - 2\psi_i + \psi_{i+1}}{h^2},$$

$$\left.\frac{\partial \psi}{\partial y}\right|_i = \frac{-\psi_{i-1} + \psi_{i+1}}{2h} \tag{15a, b}$$

The partial derivatives in z-direction are formulated similarly.

Cross-sectional Analysis of Beams Subjected to Saint-Venant Torsion

2.3   Analysis at interior nodes

2.3.1   Uniform grid

Figure 3 shows the node distribution of the beam's cross-section having equidistant nodes with spacings **Δy** and **Δz** in y- and z-direction, respectively. The node of interest **k** and the surrounding nodes are represented, whereby n, s, e, and w stand for the directions north, south, east, and west, respectively, according to the directions in the stencil. The node k may even be at the boundary of the beam, however being not at angles.
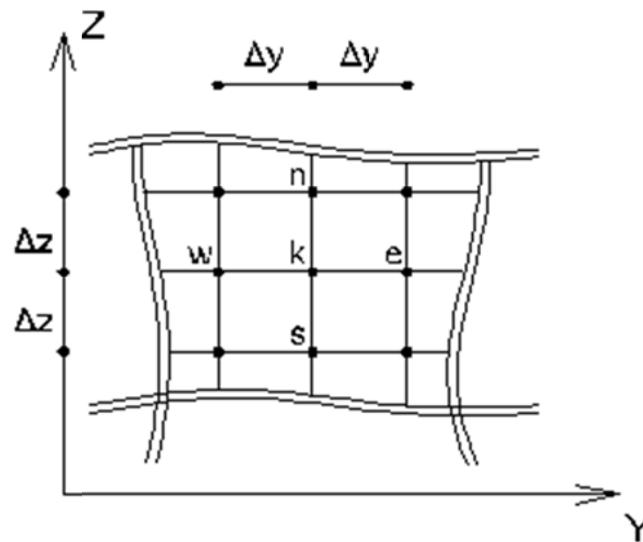

Figure 3 Node of interest **k** and its surrounding nodes for uniform grid

Given the grid spacings **Δy** = **h** and **Δz** = **λh**. The governing equation (Equation (13b-1)) at a given node can be expressed by means of a stencil using Equations (15a) as follows

$$\frac{1}{h^2}\begin{bmatrix} & \dfrac{1}{\lambda^2} & \\ 1 & \left[-2-\dfrac{2}{\lambda^2}\right] & 1 \\ & \dfrac{1}{\lambda^2} & \end{bmatrix} \times [\psi] = -2 \tag{16}$$

The shearing stresses are expressed using Equations (13b) and (15b) as follows

$$\tau_{xy} = G\frac{d\theta}{dx} \times \frac{1}{2\lambda h}\begin{bmatrix} 1 \\ [0] \\ -1 \end{bmatrix} \times [\psi], \qquad \tau_{xz} = -G\frac{d\theta}{dx} \times \frac{1}{2h}\begin{bmatrix} -1 & [0] & 1 \end{bmatrix} \times [\psi] \tag{17}$$

In the stencil notation the factor associated to the node of interest is in brackets.

Cross-sectional Analysis of Beams Subjected to Saint-Venant Torsion

2.3.2   Non-uniform grid

The distances to the node of interest k are represented in Figure 4 below
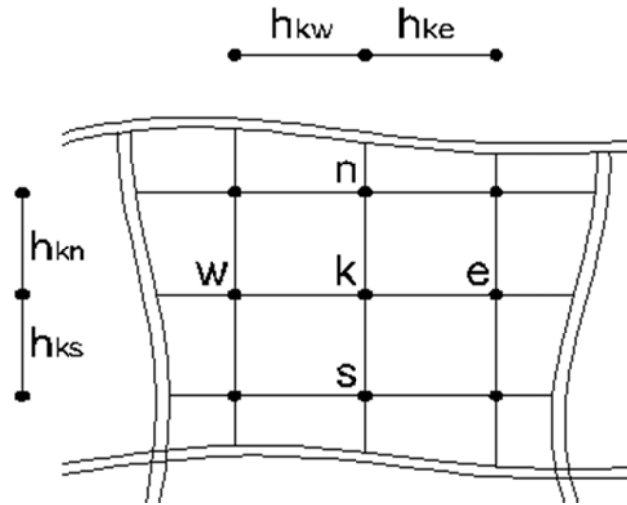

Figure 4 Node of interest **k** and its surrounding nodes for non-uniform grid

The stress function in y-direction i.e. can be described with values at grid points as follows:

$$\psi_{i-1} \times f_{i-1}(x) + \psi_i \times f_i(x) + \psi_{i+1} \times f_{i+1}(x) \tag{18a}$$

The shape functions $f_j(x)$ (j = i-1; i; i+) can be expressed using the following Lagrange interpolating polynomials

$$f_j(x) = \prod_{\substack{k=i-1 \\ k \neq j}}^{i+1} \frac{x - x_k}{x_j - x_k} \tag{18b}$$

The governing equation at node k is derived using Equations (13b-a), (18a), and (18b) as follows

$$\begin{bmatrix} & \dfrac{2}{h_{kn}\left(h_{kn}+h_{ks}\right)} & \\[2em] \dfrac{2}{h_{kw}\left(h_{kw}+h_{ke}\right)} & \left[-\dfrac{2}{h_{kw}h_{ke}} - \dfrac{2}{h_{kn}h_{ks}}\right] & \dfrac{2}{h_{ke}\left(h_{kw}+h_{ke}\right)} \\[2em] & \dfrac{2}{h_{ks}\left(h_{kn}+h_{ks}\right)} & \end{bmatrix} \times [\psi] = -2 \tag{19}$$

Cross-sectional Analysis of Beams Subjected to Saint-Venant Torsion

The shearing stresses are expressed using Equations (13b), (18a), and (18b) as follows

$$\tau_{xy} = G\frac{d\theta}{dx} \times \begin{bmatrix} \dfrac{h_{ks}}{h_{kn}\left(h_{kn} + h_{ks}\right)} \\ \left[\dfrac{1}{h_{ks}} - \dfrac{1}{h_{kn}}\right] \\ -\dfrac{h_{kn}}{h_{ks}\left(h_{kn} + h_{ks}\right)} \end{bmatrix} \times [\psi], \qquad (20a\text{-}b)$$

$$\tau_{xz} = -G\frac{d\theta}{dx} \times \begin{bmatrix} \dfrac{-h_{ke}}{h_{kw}\left(h_{kw} + h_{ke}\right)} & \left[\dfrac{1}{h_{kw}} - \dfrac{1}{h_{ke}}\right] & \dfrac{h_{kw}}{h_{ke}\left(h_{kw} + h_{ke}\right)} \end{bmatrix} \times [\psi]$$

2.4   Analysis at skew edges

Figure 5 shows the skew edge of the beam's cross-section with regular and additional nodes. The tangent **t** to the skew edge makes an angle α with the +y-axis. One additional node is associated to each edge node; therefore, the governing equation (Equation (16) or (19)) is applied at any edge node and the boundary condition $\psi = 0$ is set.
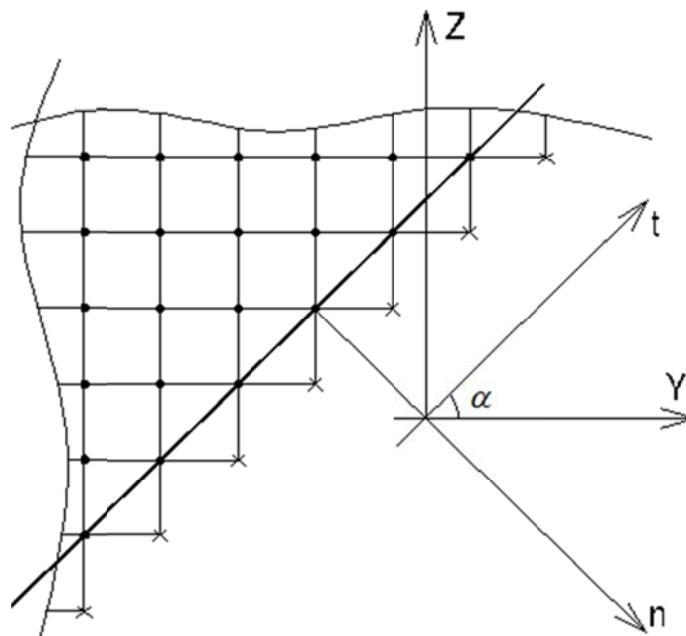

Figure 5   Skew edge of beam's cross-section with regular nodes (•) and additional nodes (×)

It is recalled that the shear stress component τ_t directed along the tangent is calculated using Equations (9a), and the shear stress component τ_{xy} and τ_{xz} using Equations (17) or (20a-b).

Cross-sectional Analysis of Beams Subjected to Saint-Venant Torsion

2.5   Analysis at beam angles

The node distribution must be such that at any position three nodes are available in both directions; so the governing equations that are formulated through the second derivatives of the stress function can be set.

2.5.1   Right angles

Figure 6 below represents angles of the beam's cross-section whereby regular nodes (•) and additional nodes (×) are represented. The unknown at each node, regular or additional, is the value of the function $\psi(y, z)$. One additional node is associated to each boundary node, at which the boundary condition $\psi = 0$ is set. The governing equations at angle nodes W, E, S, and SE are modified using Equation (15a) to account for the absence of additional nodes in z-direction; Therefore Equation (21a) is the governing equation at angles W and E, while Equation (21b) is the governing equation at angles S and SE. Alternatively, additional nodes at angles could be considered in z-direction instead.

$$\frac{1}{h^2}\begin{bmatrix} 1 & \left[-2+\dfrac{1}{\lambda^2}\right] & 1 \\ & -\dfrac{2}{\lambda^2} & \\ & \dfrac{1}{\lambda^2} & \end{bmatrix}\times[\psi]=-2, \qquad \frac{1}{h^2}\begin{bmatrix} & \dfrac{1}{\lambda^2} & \\ & -\dfrac{2}{\lambda^2} & \\ 1 & \left[-2+\dfrac{1}{\lambda^2}\right] & 1 \end{bmatrix}\times[\psi]=-2 \qquad \text{(21a-b)}$$
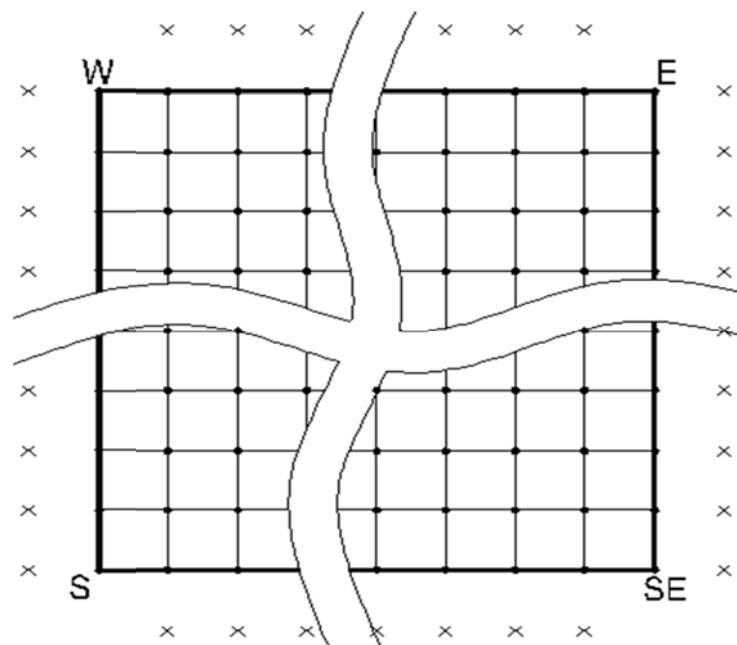

Figure 6 Angles of beam's cross-section with regular nodes (•) and additional nodes (×)

Cross-sectional Analysis of Beams Subjected to Saint-Venant Torsion

2.5.2   Various types of angles and shapes of beam's cross-sections

Examples of node distributions at various angles and shapes of beam's cross-sections are represented in Figure 7. The additional node associated to a node k is denoted by ka.
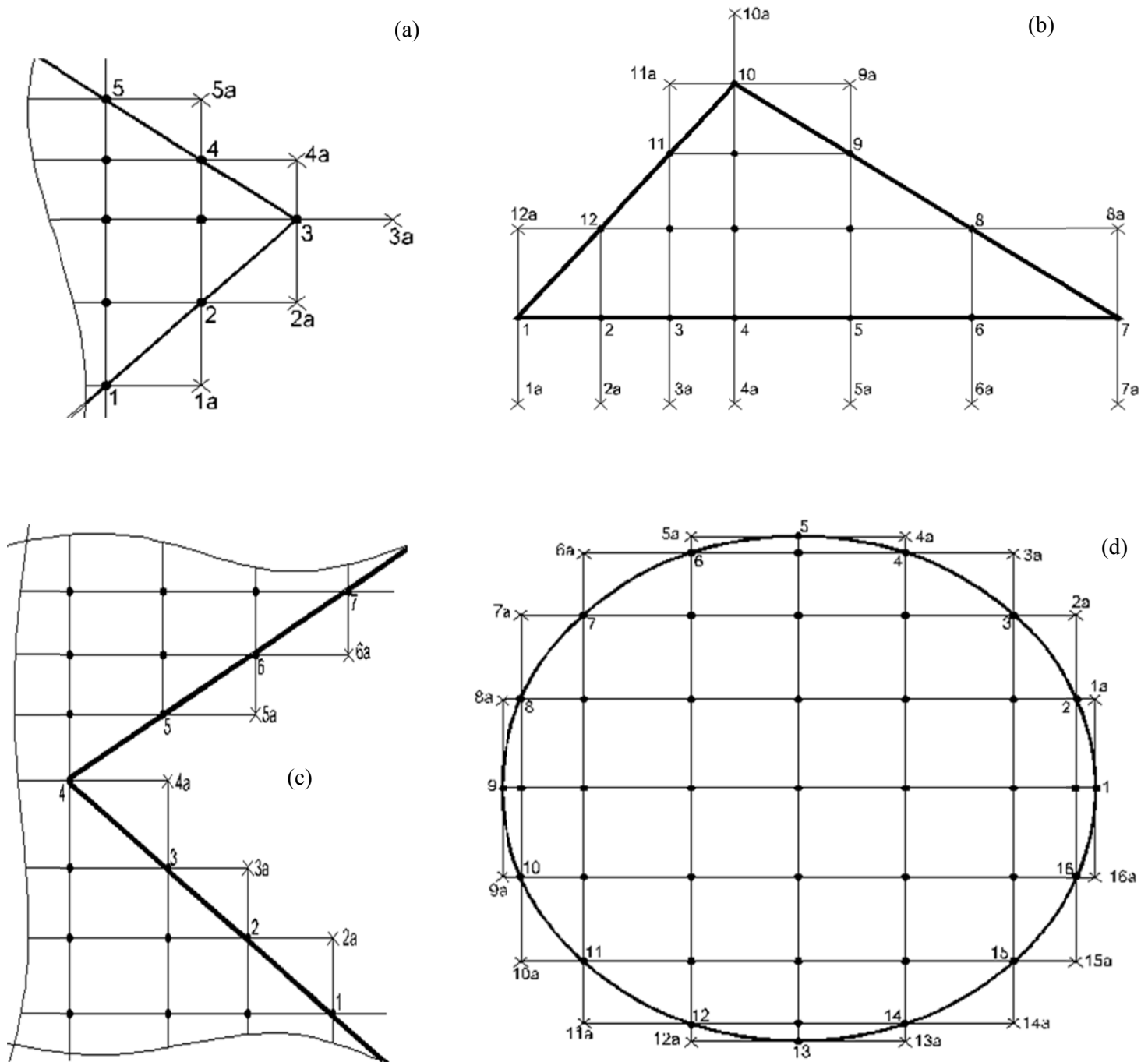

Figure 7 Examples of node distributions at various angles and shapes of beam's cross-sections

In the following the stencils may have to be modified to account for eventual non-uniform grids. Equations (16) or (19), the governing equations, are applied at any boundary node if possible. In Figure 7b, the governing equations at nodes 8

and 12 are expressed using Equation (21a); furthermore, the governing equations at nodes 1 and 11, and at nodes 7 and 9, respectively, are expressed using Equations (22a-b) as follows

$$\frac{1}{h^2}\begin{bmatrix}\dfrac{1}{\lambda^2}\\[2mm]\left[1-\dfrac{2}{\lambda^2}\right] & -2 & 1\\[2mm]\dfrac{1}{\lambda^2}\end{bmatrix}\times[\psi]=-2, \qquad \frac{1}{h^2}\begin{bmatrix}\dfrac{1}{\lambda^2}\\[2mm]1 & -2 & \left[1-\dfrac{2}{\lambda^2}\right]\\[2mm]\dfrac{1}{\lambda^2}\end{bmatrix}\times[\psi]=-2 \qquad (22a\text{-}b)$$

In Figure 7c, the governing equations at node 5 is applied using Equation (21b). In Figure 7d, the governing equations at nodes 9 and 1, respectively, are expressed using Equations (22a-b) and the governing equations at nodes 5 and 13, respectively, are expressed using Equations (21a-b).

2.6 Beams with openings

2.6.1 Openings aligned with the Cartesian coordinate system

A beam's cross-section having an opening is represented in Figure 8, together with regular nodes (●) and additional nodes (×). The opening is aligned with the Cartesian coordinate system. The unknown at regular nodes and additional nodes is the value of the stress function. The additional node associated to node k is denoted by ka.
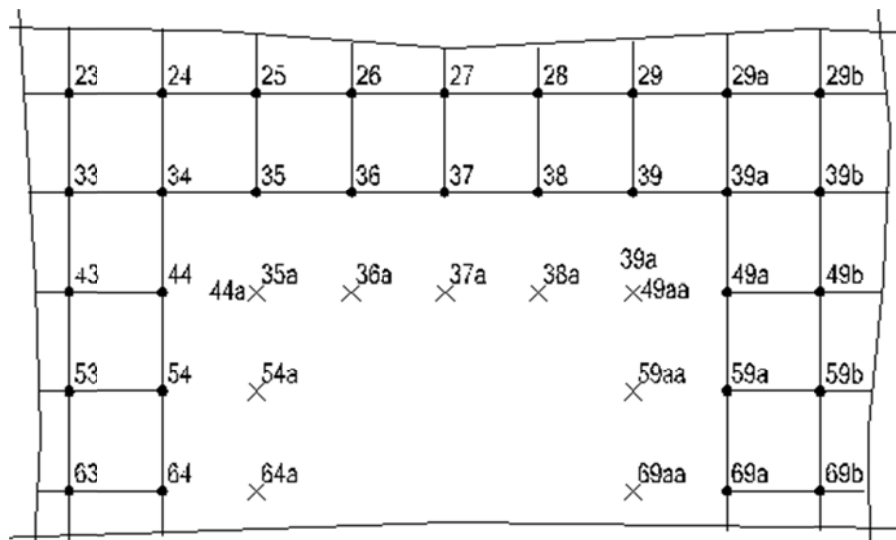

Figure 8 Beam's cross-section having an opening aligned with the Cartesian coordinate system

Similarly to Fogang [14] related to the analysis of deep beams, **it is assumed that different nodes may be at the same geometrical position**, i.e. nodes 35a and 44a, 39a and 49aa in Figure 8. The governing equations are applied to any node on the opening. The boundary conditions are ψ = constant at nodes on the opening, formulated as $\psi_k = \psi_i$

whereby i is a fixed node and k is any other node on the opening. Therefore, if boundary conditions are applied to n nodes in the opening, making n - 1 equations, then **n - 1** additional nodes should be considered in order to have as many nodes as equations. However, boundary conditions are not applied to angle nodes 34 and 39a since additional nodes are not associated to them; this corresponds to chamfering the right angles and letting the angle nodes 34 and 39a behave like interior nodes as represented in Figure 9.
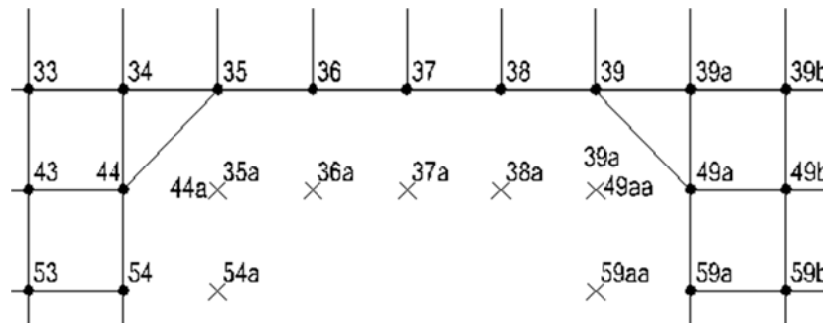
Figure 9 Beam's cross-section having an opening with chamfering of the right angles

Particular attention must be taken by the formulation of the governing equations and equations determining the shear stresses, especially in the vicinity of angle nodes; those equations at any node k involve the node ka.

2.6.2   Openings with various shapes

A beam's cross-section having an opening is represented in Figure 10, together with regular nodes (●) and additional nodes (×). The opening is not aligned with the Cartesian coordinate system.

Figure 10 Beam's cross-section having an opening of various shape

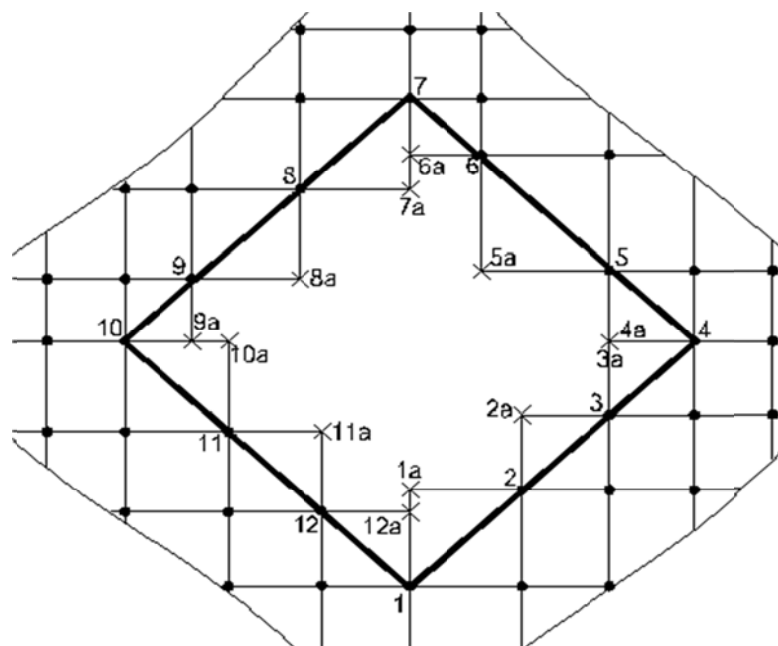**Cross-sectional Analysis of Beams Subjected to Saint-Venant Torsion**

It is further assumed that different nodes may be at the same geometrical position, i.e. nodes 4a and 3a. The governing equations are applied to any node on the opening. The boundary conditions ψ = constant are applied to any nodes on the opening since additional nodes are associated to all of them. Therefore, for Figure 10 eleven boundary conditions are applied and so eleven additional nodes should be considered in order to have as many nodes as equations. Consequently the node 12a gets suppressed. By the formulation of the governing equations and equations determining the shear stresses, especially at angle nodes; those equations at any node k involve the node ka.

2.7   Beams with thin-walled sections
2.7.1   Fundamentals of thin-walled sections

Given a beam with thin-walled section represented in Figure 11.
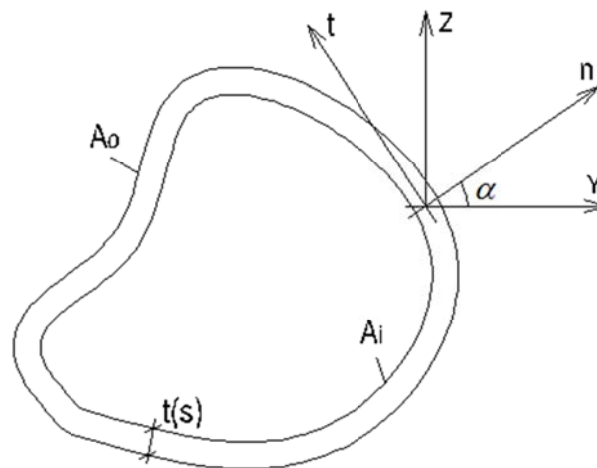
Figure 11   Beam with thin-walled section

At the one hand, the analysis of beams with single-cell thin-walled closed sections i.e. is governed by the following Bredt's [3] formulas for the shear stress τ_t at an arc coordinate s and the torsion constant I_t

$$\tau_t\left(s\right) = \frac{M_t}{2A_m t\left(s\right)}, \qquad I_t = \frac{4A_m^2}{\oint \dfrac{ds}{t\left(s\right)}} \tag{23a-b}$$

where A_m is the area enclosed by the midline of the thin-walled closed section. Bredt's formulas are derived under the assumption of a constant shear stress τ_t over the thickness whereby stresses τ_n are neglected.

At the other hand, the analysis of thin-walled open sections is governed by the following formulas

$$\tau_{max}\left(s\right) = \frac{M_t}{I_t} t\left(s\right), \qquad I_t = \frac{1}{3}\int t\left(s\right)^3 ds \tag{23c-d}$$

Cross-sectional Analysis of Beams Subjected to Saint-Venant Torsion

In the present study, the stress components τ_n and τ_t can be defined as follows using a coordinate transformation and observing Figure 2 and Equations (6),

$$\tau_n = \frac{\partial \phi}{\partial s}, \qquad \tau_t = -\frac{\partial \phi}{\partial n} \tag{24a-b}$$

Furthermore, Equations (4), (7), and (13b) are transformed as follows

$$\frac{\partial \tau_n}{\partial s} - \frac{\partial \tau_t}{\partial n} = -2G\frac{d\theta}{dx}, \qquad \frac{\partial^2 \phi}{\partial s^2} + \frac{\partial^2 \phi}{\partial n^2} = -2G\frac{d\theta}{dx}, \qquad \frac{\partial^2 \psi}{\partial s^2} + \frac{\partial^2 \psi}{\partial n^2} = -2 \tag{25a-c}$$

Let us consider continuity regions and discontinuity regions in the cross-section defined as follows: continuity regions that are away from segment ends and angles of the cross-section, are characterized by constant stress function along the arc coordinate s while discontinuity regions are segment ends and angles of the cross-section.

2.7.2 Thin-walled open sections

At an arc coordinate s the inner and outer node are denoted by si and so, respectively. Recalling that the stress function is constant along the unique boundary, the stress component τ_s at the midline at position s of thickness t(s) can be determined using Equations (15b) and (24b) as follows

$$\tau_t(s) = -\frac{\partial \phi}{\partial n} = -\frac{\phi_{so} - \phi_{si}}{t(s)} = 0 \tag{26}$$

The stress component τ_t at the midline is zero: this finding is in agreement with the analysis of thin-walled open sections. Equation (24a) shows that the stress component τ_n is zero in continuity regions while τ_t that is zero at midline can be expressed as follows using Equation (25a)

$$\tau_t(s,n) = 2G\frac{d\theta}{dx} \times n \tag{27a}$$

The stress τ_t can be formulated using the torsion constant It and the torque Mt in Equation (13c) as follows

$$\tau_t(s,n) = 2\frac{M_t}{I_t} \times n \tag{27b}$$

Equation (27b) shows that the stress component τ_t is linearly distributed over the thickness, zero at midline and maximal at the boundaries as follows

$$\tau_{t,\max}(s) = \pm 2\frac{M_t}{I_t} \times \frac{t(s)}{2} = \pm\frac{M_t}{I_t} \times t(s) \tag{27c}$$

Cross-sectional Analysis of Beams Subjected to Saint-Venant Torsion

Consequently, the maximal stresses occur at positions with greatest thickness; this finding is in agreement with the analysis of thin-walled open sections. The modified stress function ψ(s, n) defined in Equation (13a) which is zero at n = ± t(s)/2 and satisfies Equation (25c) is given by

$$\psi(s,n) = \frac{t(s)^2}{4}\left(1 - \frac{4n^2}{t(s)^2}\right)$$ (28a)

Then, the torsion constant It calculated using Equation (13d) and (28a) is

$$I_t = \frac{1}{3}\int t(s)^3\,ds$$ (28b)

Equation (28b) is a well-known formula in the analysis of thin-walled open sections.

2.7.3 Thin-walled closed sections

The analysis of closed thin-walled sections is conducted using the Bredt's [3] formulas (Equations (23a-b)). These formulas are based on the assumptions of constant shear stress τt over the thickness and neglecting the stress component τn. First, these assumptions do not satisfy the relationship between the shear stresses (Equation (4)). Second, Bredt's Equation (23a) implies that the total torque is due to the stress component τt, and as shown earlier (Equation (12f)), that is inexact. In the following, another approach for the torsional analysis of closed thin-walled sections is presented.

Single-cell thin-walled section: The stress function is taken zero along the outer boundary and ϕ_{si} along the inner one. The stress component τt at the midline at position s of thickness t(s) can be determined using Equations (15b) and (24b) as follows

$$\tau_t(s) = -\frac{\partial\phi}{\partial n} = -\frac{\phi_{so} - \phi_{si}}{t(s)} = \frac{\phi_{si}}{t(s)}$$ (29)

It is worth mentioning that ϕ_{si} corresponds to the shear flow of the Bredt's analysis. The stress component τt can also be determined using Equations (9a) as follows

$$\tau_t = \frac{\partial\phi}{\partial z}\frac{dy}{ds} - \frac{\partial\phi}{\partial y}\frac{dz}{ds} \rightarrow \tau_t ds = \frac{\partial\phi}{\partial z}dy - \frac{\partial\phi}{\partial y}dz$$ (30)

Let us perform a line integral through the midline using Equations (7), (13a), and (29-30) and the Green's theorem

$$\oint_M \tau_t ds = \oint_M \frac{\phi_{si}}{t(s)}ds = \oint_B\left[\frac{\partial\phi}{\partial z}dy - \frac{\partial\phi}{\partial y}dz\right] = \iint_A\left[-\frac{\partial^2\phi}{\partial y^2} - \frac{\partial^2\phi}{\partial z^2}\right]dydz = 2G\frac{d\theta}{dx}A_M$$

$$\rightarrow \oint_M \frac{\psi_{si}}{t(s)}ds = 2A_M \rightarrow \psi_{si} = \frac{2A_M}{\displaystyle\oint_M \frac{ds}{t(s)}}$$ (31)

Cross-sectional Analysis of Beams Subjected to Saint-Venant Torsion

where A_M is the area enclosed by the midline of the cross-section. The modified stress function $\psi(s, n)$ defined in Equation (13a) which is zero and ψ_{si} at $n = \pm t(s)/2$, respectively, and satisfies Equation (25c) is given by

$$\psi(s,n) = \psi_{si}\left(\frac{1}{2} - \frac{n}{t(s)}\right) + \frac{t(s)^2}{4}\left(1 - \frac{4n^2}{t(s)^2}\right) \tag{32a}$$

The torsion constant It is then calculated using Equations (14c), (31), and (32a) as follows

$$I_t = \frac{2AA_M}{\displaystyle\oint_M \frac{ds}{t(s)}} + \frac{1}{3}\oint_M t(s)^3 \, ds + \frac{4A_M A_i}{\displaystyle\oint_M \frac{ds}{t(s)}} \tag{32b}$$

The second term at the right-hand side of Equation (32b) can be neglected; thus Equation (32b) becomes

$$I_t = \frac{2A_M\left(A_i + A_o\right)}{\displaystyle\oint_M \frac{ds}{t(s)}} \tag{32c}$$

where A_i and A_o are the areas enclosed by the inner and the outer boundary of the cross-section, respectively, and A is the area of the cross-section material. This expression of the torsion constant looks similar to that of Bredt (Equation (23b), $A_i + A_o$ replacing $2A_M$) and coincides with it for very small thicknesses.

In continuity regions, the stress component τ_n is zero and τ_t is as follows using Equations (25a) and (29).

$$\tau_t\left(s,n\right) = 2G\frac{d\theta}{dx} \times n + \frac{\phi_{si}}{t(s)} \tag{33a}$$

Equation (33a) shows that at a position s the stress component τ_t is linearly distributed over the thickness, maximal and minimal at the boundaries. Using Equations (13c) and (31) τ_t is given by

$$\tau_{t,\max,\min}\left(s\right) = \frac{M_t}{I_t} \times \left(\pm t\left(s\right) + \frac{1}{t(s)} \times \frac{2A_M}{\displaystyle\oint_M \frac{ds}{t(s)}} \right) \tag{33b}$$

Equation (33b) shows that contrarily to Bredt's formulas the maximum shear stress in the cross-section does not necessarily occur at the position with the smallest thickness. The shear stress at the midline is as follows using Equations (13c), (29), (31), and (32c);

$$\tau_t\left(s\right) = \frac{M_t}{\left(A_i + A_o\right)t\left(s\right)}, \tag{33c}$$

it is noted that its maximal value occurs at the position with the smallest thickness; interestingly the expression looks similar to that of Bredt (Equation (23a), $A_i + A_o$ replacing $2A_M$).

Multiple-cell thin-walled section: The stress function is taken zero along the outer boundary and ϕ_{sk} along the inner boundary of a cell k. For a given cell at a position s the stress function at the inner and outer boundary are denoted by ϕ_{si} and ϕ_{so}, respectively. So, the stress component τ_t at the midline at position s of thickness t(s) is as follows

$$\tau_t(s) = -\frac{\partial \phi}{\partial n} = -\frac{\phi_{so} - \phi_{si}}{t(s)} = \frac{\phi_{si} - \phi_{so}}{t(s)} \tag{34a}$$

Equation (31) is applied at each cell through the midline using Equations (12e), (13a), and (34a); for the cell k it yields

$$\oint_k \frac{\psi_{si} - \psi_{so}}{t_k(s)} ds = 2A_{Mk} \tag{34b}$$

where A_{Mk} is the area enclosed by the midline of the cell k. Let the cell k of thickness $t_k(s)$ be bordered by q cells of thickness $t_q(s)$; Equation (34b) applied at the cell k is

$$\psi_k \oint_k \frac{ds}{t_k(s)} - \sum_q \psi_q \int \frac{ds}{t_q(s)} = 2A_{Mk} \tag{34c}$$

So, the values ψ_k of the modified stress function at the inner boundaries of the cells can be determined from the system of linear equations (34c). $\psi(s, n)$ defined in Equation (13a) with values ψ_{so} and ψ_{si} at $n = \pm t(s)/2$, respectively, which satisfies Equation (25c) is given by

$$\psi(s,n) = \psi_{si}\left(\frac{1}{2} - \frac{n}{t(s)}\right) + \psi_{so}\left(\frac{1}{2} + \frac{n}{t(s)}\right) + \frac{t(s)^2}{4}\left(1 - \frac{4n^2}{t(s)^2}\right) \tag{35a}$$

The torsion constant It is then calculated using Equation (14c) and (35a)

$$I_t = \int (\psi_{si} + \psi_{so})t(s)ds + \frac{1}{3}\int t(s)^3 ds + 2\sum_k \psi_k A_{ik} \tag{35b}$$

where A_{ik} is the area enclosed by the inner boundary of the cell k. The first integral in Equation (35b) is rewritten as

$$\int (\psi_{si} + \psi_{so})t(s)ds = \sum_k \psi_k A_k \tag{35c}$$

Cross-sectional Analysis of Beams Subjected to Saint-Venant Torsion

where A_k is the area of the cross-section material associated to the cell k. The second term at the right-hand side of Equation (35b) can also be neglected; substituting Equation (35c) into (35b) yields

$$I_t = \sum_k \psi_k \left(A_{ik} + A_{ok} \right) \tag{35d}$$

where A_{ok} is the area enclosed by the outer boundary of the cell k. As an example the analysis of a three-cell thin-walled section is presented in Appendix B.

In continuity regions, the stress component τ_n is zero and τ_t is as follows using Equations (25a) and (34a)

$$\tau_t \left(s, n \right) = 2G \frac{d\theta}{dx} \times n + \frac{\phi_{si} - \phi_{so}}{t(s)} = \frac{M_t}{I_t} \times \left(2n + \frac{\psi_{si} - \psi_{so}}{t(s)} \right) \tag{36a}$$

Similarly to the single-cell thin-walled section, the stress component τ_t at a position s is linearly distributed over the thickness, maximal and minimal at the boundaries as follows

$$\tau_{t,\max,\min} \left(s \right) = \frac{M_t}{I_t} \times \left(\pm t \left(s \right) + \frac{\psi_{si} - \psi_{so}}{t(s)} \right) \tag{36b}$$

For a segment of the beam's cross-section bordered by cells j and k and having the thickness t_{jk}, the shear stresses can be calculated using Equation (36b) either from the cell j or from the cell k; $\tau_{p,i}$ and $\tau_{p,o}$ being the stresses at the inner and outer boundary of the cell p (p = j, k), respectively, it yields

$$\tau_{j,i} = \frac{M_t}{I_t} \times \left(-t_{jk} + \frac{\psi_j - \psi_k}{t_{jk}} \right), \qquad \tau_{j,o} = \frac{M_t}{I_t} \times \left(t_{jk} + \frac{\psi_j - \psi_k}{t_{jk}} \right)$$

$$\tau_{k,i} = \frac{M_t}{I_t} \times \left(-t_{jk} + \frac{\psi_k - \psi_j}{t_{jk}} \right), \qquad \tau_{k,o} = \frac{M_t}{I_t} \times \left(t_{jk} + \frac{\psi_k - \psi_j}{t_{jk}} \right) \tag{36c}$$

It is noted as expected that $\tau_{j,i} = -\tau_{k,o}$ and $\tau_{j,o} = -\tau_{k,i}$.

Cross-sectional Analysis of Beams Subjected to Saint-Venant Torsion

2.8   Warping of the cross-section

In the following the cross-sections are assumed free to warp. For a given cross-section and torque the values of the stress function $\psi(y,z)$ were determined according to previous sections. Substituting Equations (3a-b) into (5) yields

$$\frac{\partial^2 u}{\partial y^2} + \frac{\partial^2 u}{\partial z^2} = 0 \tag{37a}$$

Let the outer normal to the boundary make an angle α with the +y-axis (see Figure 2). The boundary conditions are such that the shearing stress component at the boundary directed along the outer normal is zero from the condition of stress free outer surfaces; this shear stress is expressed using Equations (9b) and (3a-b)

$$\tau_n = G\left(\frac{\partial u}{\partial y} - (z - z_T)\frac{d\theta}{dx}\right)\cos\alpha + G\left(\frac{\partial u}{\partial z} + (y - y_T)\frac{d\theta}{dx}\right)\sin\alpha = 0 \tag{37b}$$

Equation (37b) can be rewritten using (13c)

$$G\left(\frac{\partial u}{\partial y}\cos\alpha + \frac{\partial u}{\partial z}\sin\alpha\right) + \frac{M_t}{I_t}\left[(y - y_T)\sin\alpha - (z - z_T)\cos\alpha\right] = 0 \tag{37c}$$

Equation (37a) is the governing equation which is applied at any node of the cross-section and Equation (37c) is the boundary condition. For convenience the node distribution is taken the same as that for the stress function. So, the governing equation (Equation (37a)) is expressed similar to that of the stress function (Equations (16) and (19)); however, zero is put in place of the right-hand side of the latter equations. A modified warping U is defined as $U = GI_t/M_t \times u$; therefore, Equations (37a) and (37c) become

$$\frac{\partial^2 U}{\partial y^2} + \frac{\partial^2 U}{\partial z^2} = 0$$

$$\frac{\partial U}{\partial y}\cos\alpha + \frac{\partial U}{\partial z}\sin\alpha + (y - y_T)\sin\alpha - (z - z_T)\cos\alpha = 0 \tag{38a-b}$$

In Equation (38b) the derivatives of U are expressed using the stencils in Equations (17) and (20a-b). **A kinematic boundary condition is needed for solving the warping problem;** therefore, at the center of torsion T (y_T, z_T) (equivalent to the shear center) or at another point suitably chosen (i.e. a point in the symmetry axis) the warping is set to zero and the governing equation is not applied.

Beam with circular cross-section: the center of torsion is at $y_T = z_T = 0$, and the boundary is defined by $y = R\cos\alpha$, and $z = R\sin\alpha$. It results that both governing equation and boundary condition ($\partial U/\partial y \times \cos\alpha + \partial U/\partial z \times \sin\alpha = 0$) are homogeneous differential equations and consequently the warping is zero.

Cross-sectional Analysis of Beams Subjected to Saint-Venant Torsion

3   Results and discussions

3.1   Torsion of beam with rectangular cross-section

The elastic torsional behavior of a beam with rectangular cross-section was analyzed. The dimensions of the cross-section in y- and z-directions are denoted by a and b, respectively. The torsion constant $It = k_1 ba^3$ and the maximal shear stress $\tau_{max} = ka\, Gd\theta/dx$ are determined, depending on the ratio b/a. A 4×4, 8×8, and 12×12 element mesh are considered. Details of the analysis and results are presented in Appendix A and in the supplementary material "Torsion of beam with rectangular cross-section." Table 1 lists the results obtained with Timoshenko [15] using the membrane analogy (exact results) and those obtained in the present study.

Table 1   Coefficients of the torsion constant and maximal shear stress

	b/a =									
	1.00		**1.50**		**2.00**		**3.00**		**10.00**	
	k_1	**k**	**k_1**	**k**	**k_1**	**k**	**k_1**	**k**	**k_1**	**k**
	Solution by Timoshenko [15] (exact results)									
	0.141	0.675	0.196	0.848	0.229	0.930	0.263	0.985	0.312	1.000
	Present study (Finite Difference Method)									
4 × 4 elements	0.133	0.688	0.185	0.838	0.215	0.913	0.243	0.971	0.270	1.000
8 × 8 elements	0.140	0.677	0.194	0.844	0.227	0.925	0.260	0.982	0.298	1.000
12 × 12 elements	0.140	0.676	0.195	0.846	0.228	0.928	0.262	0.984	0.305	1.000

As Table 1 shows, the results using FDM show good agreement with the exact results, and the accuracy is increased through a grid refinement. For high values of b/a, the torsion constant It is equal to $1/3 \times ba^3$.

The warping is calculated for a beam with dimensions a = b = 1.0m for a unity torque, whereby a 12×12 mesh with spacings $\Delta y = \Delta z = h$ is considered. Recalling that $y_T = z_T = 0$ for the rectangular cross-section, the boundary conditions are set observing that at the edges $y = \pm a/2$ the outer normal to the boundary makes an angle $\alpha = 0$ and π, respectively, with the +y-axis and at the edges $z = \pm b/2$ makes an angle $\alpha = \pi/2$ and $3\pi/2$, respectively. Equation (38b) is then formulated as $U_e - U_w - 2hz = 0$ and $U_n - U_s + 2hy = 0$ at the edges $y = \pm a/2$ and $z = \pm b/2$, respectively. Details of the results are presented in the above mentioned supplementary material. The factored warping $G \times u = U/It$ ($It = 0.141$ m^4) is given in Table 2.

Cross-sectional Analysis of Beams Subjected to Saint-Venant Torsion

Table 2   Factored warping $G \times u$ for a beam with dimensions a = b = 1.0m and Mt = 1.0 MNm

-0.151	0.104	0.202	0.212	0.168	0.091	0.000	-0.091	-0.168	-0.212	-0.202	-0.104	0.151
-0.270	-0.064	0.048	0.090	0.085	0.049	0.000	-0.049	-0.085	-0.090	-0.048	0.064	0.270
-0.306	-0.139	-0.035	0.017	0.031	0.022	0.000	-0.022	-0.031	-0.017	0.035	0.139	0.306
-0.279	-0.152	-0.068	-0.019	0.003	0.006	0.000	-0.006	-0.003	0.019	0.068	0.152	0.279
-0.208	-0.123	-0.064	-0.027	-0.008	-0.001	0.000	0.001	0.008	0.027	0.064	0.123	0.208
-0.111	-0.068	-0.037	-0.018	-0.007	-0.002	0.000	0.002	0.007	0.018	0.037	0.068	0.111
0.000	0.000	0.000	0.000	0.000	0.000	0.000	0.000	0.000	0.000	0.000	0.000	0.000
0.111	0.068	0.037	0.018	0.007	0.002	0.000	-0.002	-0.007	-0.018	-0.037	-0.068	-0.111
0.208	0.123	0.064	0.027	0.008	0.001	0.000	-0.001	-0.008	-0.027	-0.064	-0.123	-0.208
0.279	0.152	0.068	0.019	-0.003	-0.006	0.000	0.006	0.003	-0.019	-0.068	-0.152	-0.279
0.306	0.139	0.035	-0.017	-0.031	-0.022	0.000	0.022	0.031	0.017	-0.035	-0.139	-0.306
0.270	0.064	-0.048	-0.090	-0.085	-0.049	0.000	0.049	0.085	0.090	0.048	-0.064	-0.270
0.151	-0.104	-0.202	-0.212	-0.168	-0.091	0.000	0.091	0.168	0.212	0.202	0.104	-0.151

.

The distortions are zero in the symmetry axes of the beam and greatest in the sides between the axis and the angles.

3.2   Torsion of beam with rectangular cross section having an opening

The torsional analysis of a beam with rectangular cross section having an opening, as represented in Figure 12, was conducted. The dimensions of the cross section in y- and z-directions are denoted by a and b, respectively. The opening was centered to the cross section with dimensions a/2 and b/2 in y- and z-directions, respectively.
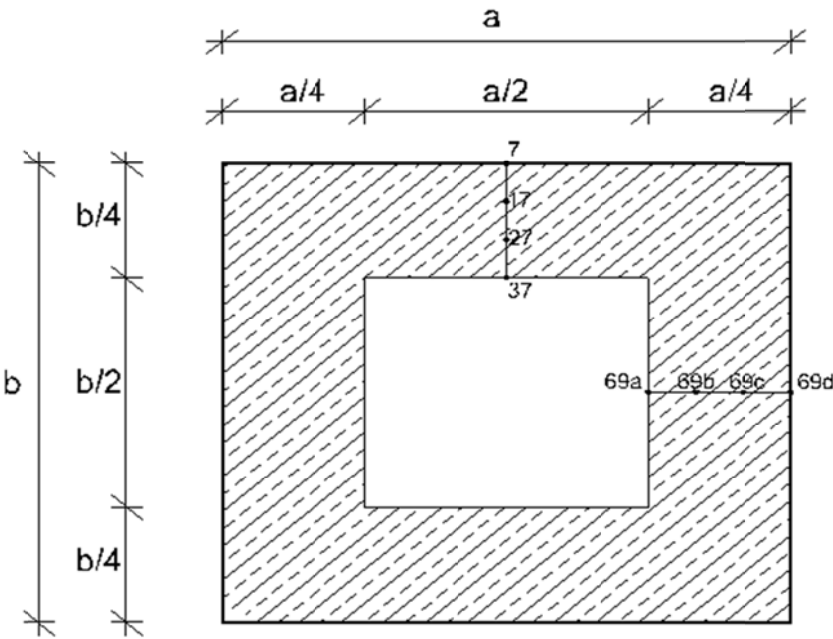

Figure 12 Beam with rectangular cross section having an opening

Cross-sectional Analysis of Beams Subjected to Saint-Venant Torsion

The shear stresses $\tau = k \times G d\theta/dx$ are calculated at the middle of the sides at nodes 7, 17, 27, and 37, and nodes 69a, 69b, 69c, and 69d, depending on the ratio b/a, whereby a = 1.0m. A 12 × 12 mesh was considered. Details of the results are presented in the supplementary material "Torsion of beam with rectangular cross section having an opening." Table 2 lists the results obtained in this study for a torque Mt = 1.0 kNm.

Table 2   Coefficients of shear stresses

	Node	b/a =					
	Node	0.25	0.50	1.00	1.50	2.00	3.00	5.00
Shear stress τ_{xy}	7	-0.162	-0.284	-0.372	-0.409	-0.448	-0.538	-0.712
	17	-0.120	-0.201	-0.206	-0.162	-0.124	-0.079	-0.043
	27	-0.079	-0.118	-0.040	0.085	0.199	0.380	0.625
	37	-0.037	-0.034	0.127	0.335	0.532	0.880	1.459
Shear stress τ_{xz}	69a	-0.135	-0.138	-0.127	-0.195	-0.330	-0.723	-1.843
	69b	-0.016	0.012	0.040	-0.027	-0.162	-0.556	-1.676
	69c	0.063	0.147	0.206	0.142	0.006	-0.389	-1.509
	69d	0.189	0.299	0.372	0.310	0.174	-0.222	-1.342
Stress function in the opening		0,0062	0.0199	0.0307	0.0143	-0.0195	-0.1182	-0.3981

For ratios b/a = 3.0 and 5.0, the shear stresses τ_{xz} over the entire thickness (nodes 69a, 69b, 69c, and 69d) are negative and consequently caused a shear flow in the opposite direction of the torque; this result is not consistent with a proper torsional behavior of the beam. Furthermore, it is noted that this situation coincides with negative values of stress function in the opening. Therefore, it can be concluded that for negative values of the stress function in the opening shear flows in the opposite direction of the torque occur; the grid must then be refined in order to have reliable results.

So, another calculation is conducted for the ratios b/a = 2.0 (12 × 24 mesh) and 3.0 (12 × 36 mesh) with grid spacings $\Delta z = \Delta y$. The results are presented in the above mentioned supplementary material and listed in Table 2a.

Table 2a   Coefficients of shear stresses for b/a = 2.0 and 3.0

b/a	Stress function in the opening	\multicolumn{3}{c}{Shear stress τ_{xy}}			\multicolumn{4}{c}{Shear stress τ_{xz}}			
		7	27 37	47 67	67 97	129a 189a	129b 189b	129c 189c	129d 189d
2.0	0.0100	-0.490	-0.175	0.130	0.459	-0.211	-0.044	0.124	0.291
3.0	-0.0107	-0.603	-0.175	0.192	0.657	-0.293	-0.126	0.040	0.207

Cross-sectional Analysis of Beams Subjected to Saint-Venant Torsion

For b/a = 3.0 the results are better (values of stress function from -0.1182 to -0.0107) but the mesh is still to improve in order to have a positive stress function in the opening.

3.3 Torsion of a beam with thin-walled sections

The elastic torsional behavior of a beam with closed thin-walled sections, as represented in Figure 13, was analyzed. The dimensions of the cross-section in y- and z-directions are denoted by a = 1.0m and b = 1.0m, respectively. The thickness t is chosen a/6, a/8, a/10, a/15, and a/20.
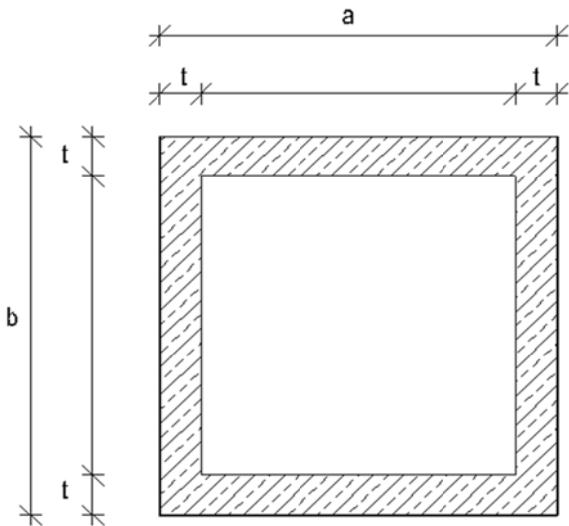
Figure 13 Beam with rectangular thin-walled section

The shear stresses τ_t are determined for a torque Mt = 1.0 kNm for numerous values of thicknesses. Details of the results are presented in the supplementary material "Torsion of beam with thin-walled sections." The results obtained in the present study are compared to those using Bredt's formulas (Equations (23a-b)) and are listed in Table 3.

Table 3   Shear stresses and torsion constant for the thin-walled closed section

		t =				
		a/6	**a/8**	**a/10**	**a/15**	**a/20**
Shear stress τ_t Bredt		4.32	5.22	6.17	8.61	11.08
Shear stresses τ_t	**Outer boundary**	5.82	6.58	7.45	9.79	12.21
	Midline	4.15	5.12	6.10	8.57	11.05
	Inner boundary	2.49	3.66	4.74	7.34	9.89
Torsion Constant It (Bredt)		0.0965	0.0837	0.0729	0.0542	0.0429
Torsion Constant It (Present study)		0.1003	0.0854	0.0738	0.0545	0.0430

The shear stresses in this study vary linearly over the thickness. As Table 3 shows, this paper presents values of shear stresses at midline close to those of Bredt but the maximal values are higher. It is noted that for very small values of thickness, the results at midline converge towards those of Bredt.

3.4   Torsion of a symmetrical beam with double-cell thin-walled section

The torsional behavior of a beam with symmetrical double-cell thin-walled section, as represented in Figure 14, was analyzed. The thicknesses are tk, k = 1 to 4.
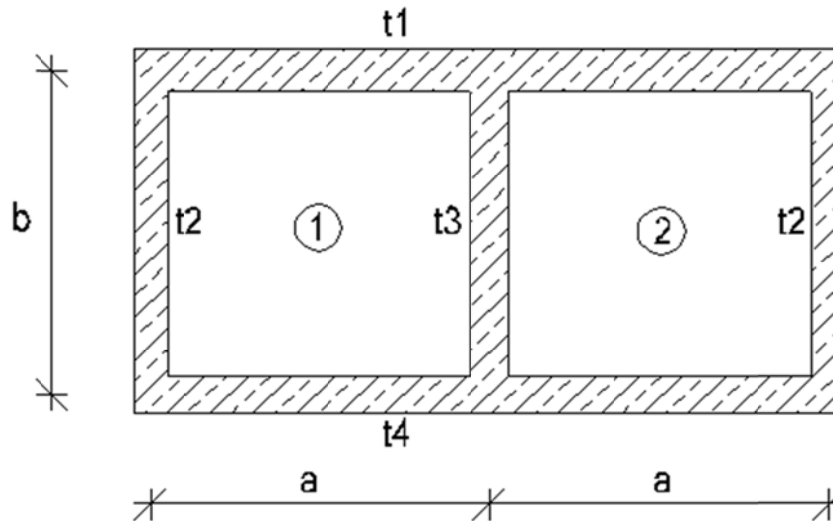
Figure 14 Beam with double-cell thin-walled section

Let ψ_1 and ψ_2 be the values of the modified stress function at the inner boundaries of the cells 1 and 2, respectively; they are calculated using Equation (34c) and the torsion constant is determined using Equation (35d)

$$\psi_1 = \psi_2 = \frac{2A_{M1}}{\dfrac{a}{t_1} + \dfrac{b}{t_2} + \dfrac{a}{t_4}}, \qquad I_t = 2\psi_1\left(A_{i1} + A_{o1}\right) \tag{39}$$

$$A_{M1} = A_{M2} = ab, \qquad A_{i1} = \left(b - \frac{t_1}{2} - \frac{t_4}{2}\right)\left(a - \frac{t_2}{2} - \frac{t_3}{2}\right), \qquad A_{o1} = \left(b + \frac{t_1}{2} + \frac{t_4}{2}\right)\left(a + \frac{t_2}{2} + \frac{t_3}{2}\right)$$

The results show that contrarily to Bredt's analysis the central web (thickness t3) contributes to the torsional stiffness and to the shear stresses; the stress distribution is linear and odd with respect to the midline with maximal and minimal value

$$\tau_{t,\max,\min} = \pm \frac{M_t}{I_t} t_3 \tag{40a}$$

The maximal and minimal values in other segments are obtained using Equation (36b), with k = 1, 2, and 4

$$\tau_{t,\max,\min} = \frac{M_t}{I_t} \times \left(\pm t_k + \frac{\psi_1}{t_k}\right) \tag{40b}$$

Cross-sectional Analysis of Beams Subjected to Saint-Venant Torsion

4 Conclusion

The FDM-based model developed in this paper enables, with certain easiness, the elastic analysis of beams subjected to Saint-Venant torsion. The results showed that the calculations, as described in this paper, yield accurate results. Beams with thin-walled sections were also analyzed and closed form solutions were presented; these solutions which account for the linear distribution of the shear stresses over the thickness can be regarded as an improvement of the Bredt's analysis.

The following aspect was not addressed in this study but could be analyzed with the model in future research:

✓   Analysis of beams with thin-walled sections using FDM

Appendix A   Beam with rectangular cross-section

Given a beam with rectangular cross-section and known values of ψ. The integral $\int\psi dy dz$ needed for the torsion constant It is determined here. The grid spacings in y- and z-direction are denoted by Δy and Δz, respectively. The cross-section is divided in rectangles around grid points, as represented in Figure 15.
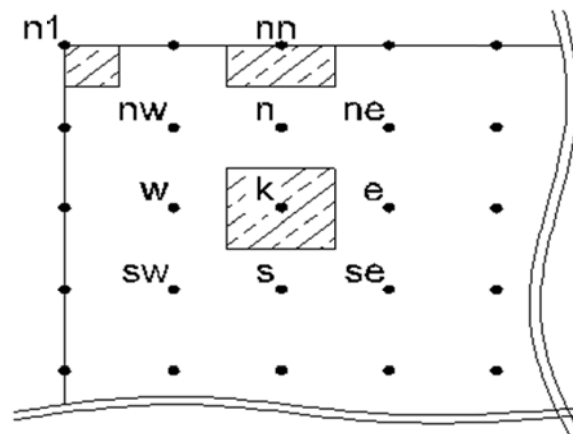

Figure 15 Rectangles for the calculation of the torsion constant

Cross-sectional Analysis of Beams Subjected to Saint-Venant Torsion

Given the rectangle bounded by nodes k, e, s, and se in Figure 15. The stress function $\psi(y,z)$ is approximated as follows

$$\psi(y,z) = \psi_k f_k(y,z) + \psi_e f_e(y,z) + \psi_s f_s(y,z) + \psi_{se} f_{se}(y,z) \tag{A1}$$

The shape function $f_e(y,z)$ i.e. can be expressed as follows

$$f_e(y,z) = \frac{yz}{\Delta y \times \Delta z} \tag{A2}$$

Using Equations (A1) and (A2), the integral for the rectangle of interest is

$$\iint \psi \, dydz = \frac{1}{4}\left(\psi_k + \psi_e + \psi_s + \psi_{se}\right) \times \Delta y \times \Delta z \tag{A3}$$

Using Equation (A3) for a uniform grid, $\int \psi dydz$ on a rectangle around an interior node (node k) is $\psi_k \Delta y \Delta z$.

Similarly, using Equation (A3) and recalling that the values of ψ are zero along the boundary, the integral for a

rectangle around a boundary node (node nn) is $1/8 \times \psi_n \Delta y \Delta z$, and for a rectangle around an angle node (node n1)

$1/64 \times \psi_{nw} \Delta y \Delta z$.

Appendix B   Three-cell thin-walled section

Given the three-cell thin-walled section represented in Figure 16, with thicknesses tk, k = 1 to 8. Let ψ_1, ψ_2, and ψ_3 be

the values of the modified stress function at the inner boundaries of the cells 1, 2, and 3, respectively.
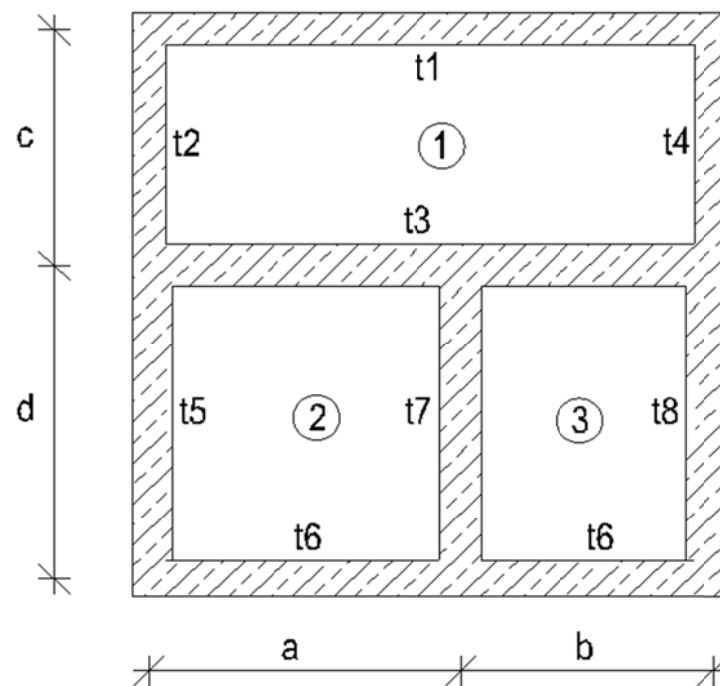

Figure 16 Three-cell thin-walled section

Cross-sectional Analysis of Beams Subjected to Saint-Venant Torsion

The areas A_{Mk}, A_{ik}, and A_{ok} with k = 1, 2, and 3 are as follows

$$A_{M1} = (a+b)c, \quad A_{i1} = \left(a+b-\frac{t_2}{2}-\frac{t_4}{2}\right)\left(c-\frac{t_1}{2}-\frac{t_3}{2}\right), \quad A_{o1} = \left(a+b+\frac{t_2}{2}+\frac{t_4}{2}\right)\left(c+\frac{t_1}{2}+\frac{t_3}{2}\right)$$

$$A_{M2} = ad, \quad A_{i2} = \left(a-\frac{t_5}{2}-\frac{t_7}{2}\right)\left(d-\frac{t_3}{2}-\frac{t_6}{2}\right), \quad A_{o2} = \left(a+\frac{t_5}{2}+\frac{t_7}{2}\right)\left(d+\frac{t_3}{2}+\frac{t_6}{2}\right) \quad \text{(B1)}$$

$$A_{M3} = bd, \quad A_{i3} = \left(b-\frac{t_7}{2}-\frac{t_8}{2}\right)\left(d-\frac{t_3}{2}-\frac{t_6}{2}\right), \quad A_{o3} = \left(b+\frac{t_7}{2}+\frac{t_8}{2}\right)\left(d+\frac{t_3}{2}+\frac{t_6}{2}\right)$$

Equation (34c) applied at each cell as follows yields the values ψ_k.

$$\psi_1\left[\frac{a+b}{t_1}+\frac{c}{t_2}+\frac{a+b}{t_3}+\frac{c}{t_4}\right]-\psi_2\frac{a}{t_3}-\psi_3\frac{b}{t_3} = 2A_{M1}$$

$$\psi_2\left[\frac{a}{t_3}+\frac{d}{t_5}+\frac{a}{t_6}+\frac{d}{t_7}\right]-\psi_1\frac{a}{t_3}-\psi_3\frac{d}{t_7} = 2A_{M2} \quad \text{(B1)}$$

$$\psi_3\left[\frac{b}{t_3}+\frac{d}{t_7}+\frac{b}{t_6}+\frac{d}{t_8}\right]-\psi_1\frac{b}{t_3}-\psi_2\frac{d}{t_7} = 2A_{M3}$$

Then the torsion constant and the shear stresses are calculated using Equations (35d) and (36c), respectively.

References

[1]   Fogang, V. Euler-Bernoulli Beam Theory: First-Order Analysis, Second-Order Analysis, Stability, and Vibration Analysis Using the Finite Difference Method. Preprints 2021, 2021020559 (doi: 10.20944/preprints202102.0559.v3).

[2]   Saint-Venant, B. Mémoires savants étrangers, vol. 14, 1855

[3]   Bredt, R. V.D.I., vol. 40, p. 815, 1896

[4]   Prandtl, L. Physik. Z., vol. 4, 1903.

[5]   Ritz, W. J. reine angew. Math., vol. 135, 1908

[6]   Trefftz, E. Proc. Second Intern. Congr. Applied Mech., Zürich, 1926, p.131

[7]   Pluzsik, A., Kollar, L.P. Torsion of closed section, orthotropic, thin-walled beams. IJSS, Volume 43, Issue 17, August 2006, Pages 5307-5336. https://doi.org/10.1016/j.ijsolstr.2005.08.001

Cross-sectional Analysis of Beams Subjected to Saint-Venant Torsion

[8] Pan, W.-H., Zhao, C.-H., Tian, Y., Lin, K.-Q. Exact Solutions for Torsion and Warping of Axial-Loaded Beam-Columns Based on Matrix Stiffness Method. Nanomaterials 2022, 12, 538. https://doi.org/10.3390/nano12030538

[9] Pavazza, R., Matoković, A., Vukasović M. 2022. A theory of torsion of thin-walled beams of arbitrary open sections with influence of shear, Mechanics Based Design of Structures and Machines, 50:1, 206-241, DOI: 10.1080/15397734.2020.1714449

[10] Choi, S., Kim, Y. Y. Higher-order Vlasov torsion theory for thin-walled box beams. IJMS, Volume 195, 1 April 2021, 106231. https://doi.org/10.1016/j.ijmecsci.2020.106231

[11] Amulu, C. P., Ezeagu, C. A. Experimental and Analytical Comparison of Torsion, Bending Moment and Shear Forces in Reinforced Concrete Beams Using BS 8110, Euro Code 2 and ACI 318 Provisions. NIJOTECH, Vol. 36, No. 3, July 2017, pp. 705 – 711. http://dx.doi.org/10.4314/njt.v36i3.7

[12] Tran, D.-B. (2021). Torsional Shear Stress in Prismatic Beams With Arbitrary Cross-Sections Using Finite Element Method. *Stavební Obzor - Civil Engineering Journal*, 30(2). https://doi.org/10.14311/CEJ.2021.02.0030

[13] Dieker, S., Reimerdes, H-G. Elementare Festigkeitslehre im Leichtbau. Donat Verlag, Bremen. 1992. ISBN 3-924444-58-7

[14] Fogang, V. Two-Dimensional Stress Analysis of Isotropic Deep Beams Using the Finite Difference Method. Preprints 2022, 2022020070 (doi: 10.20944/preprints202202.0070.v1).

[15] Timoshenko, S., Goodier, J. N. Theory of elasticity. McGraw-Hill Book Company, Inc., New York, 2nd edition, 1951